The Influence of Various Cerebral and Extracerebral Pathologies on Apparent Diffusion Coefficient Values in the Fetal Brain

Nadja Schönberg, Christian Weisstanner, Roland Wiest, Harald M. Bonél, Eike I. Piechowiak, Jennifer L. Cullmann, Luigi Raio, Manuela Pastore-Wapp, Nedelina Slavova

From the Department of Radiology and Nuclear Medicine, Winterthur Canton Hospital, Winterthur, Switzerland (NS); Institute of Diagnostic and Interventional Neuroradiology, Bern University Hospital, Bern, Switzerland (CW, RW, EIP, NS); Department of Diagnostic, Interventional and Paediatric Radiology, Bern University Hospital, Bern, Switzerland (HMB, JLC); Department of Obstetrics and Gynaecology, Bern University Hospital, Bern, Switzerland (LR); and Support Centre for Advanced Neuroimaging (SCAN), Institute of Diagnostic and Interventional Neuroradiology, Bern University Hospital, Bern, Switzerland (MPW).

ABSTRACT

BACKGROUND AND PURPOSE: **The changing MRI signal accompanying brain maturation in fetal brains can be quantified on apparent diffusion coefficient (ADC) maps. Deviations from the natural course of ADC values may reflect structural pathology. The purpose of this study was to determine the influence of fetal pathologies on the ADC values in different regions of the fetal brain and their evolution with increasing gestational age.**

METHODS: **This was a retrospective study of 291 fetuses evaluated between the 14th and the 40th week of gestation using diffusion-weighted imaging (DWI). Fetuses with normal MRI findings but sonographically suspected pathology or fetuses with abnormalities not affecting the brain were analyzed in the control group and compared to fetuses suffering from different pathologies like hydrocephalus/ventriculomegaly, brain malformations, infections, ischemia/hemorrhage, diaphragmatic hernias, and congenital heart disease. Pairwise ADC measurements in each side of the white matter (WM) of the frontal, parietal, and occipital lobes, in the basal ganglia and the cerebellum, as well as a single measurement in the pons were performed and were plotted against gestational age.**

RESULTS: **In the control group, brain maturation followed a defined gradient, resulting in lower ADC values in the most mature regions. Each disorder group experienced abnormal patterns of evolution of the ADC values over time deviating from the expected course.**

CONCLUSIONS: **The ADC values in different regions of the fetal brain and their evolution with increasing gestational age are influenced by pathologies compromising the cerebral maturation.**

Keywords: ADC, fetal MRI, brain, maturation, cerebral pathologies.

Acceptance: Received January 24, 2020. Accepted for publication April 30, 2020.

Correspondence: Address correspondence to Nedelina Slavova, Department of Diagnostic and Interventional Neuroradiology, University Hospital of Bern, Bern, Switzerland, Freiburgstrasse 8, 3010 Bern. E-mail: Nedelina.Slavova@insel.ch

NSc and CW contributed equally to the study
NSl and MPW share senior authorship

Acknowledgement and Disclosure: All authors declare no external funding source. The authors declare no financial conflicts-of-interests.

J Neuroimaging 2020;30:477-485.
DOI: 10.1111/jon.12727

Introduction

MRI has proved to be a valuable method in the assessment of sonographically suspected fetal pathology. For example, ischemia, cortical malformations, infections, as well as normal brain development can be demonstrated by diffusion-weighted imaging (DWI).[1-4] Various studies have shown that the changing MR signal accompanying brain maturation in fetal and neonatal brains can be quantified on apparent diffusion coefficient (ADC) maps,[3,5-9] whereas water diffusivity decreases with ongoing maturation as a result of progressing myelination with increasing lipid content and tissue density, formation of new synapses, fiber organization into bundles, and decreasing water content. Thus, deep ADC values are expected in cell-dense, highly organized tissues with little interstitial fluid.[1,3,5-7,10] Therefore, deviations from the natural course of these values may reflect structural pathology.[10-12] Recent studies have found that ADC calculation is reproducible method for radiologists at different gestational ages.[13,14] ADC is equivalent to mean diffusivity (MD) and is a rotationally invariant quantity obtained from 3 orthogonal measurements for time-considerations.[15,16] MD is affected by the cellular density of a voxel, or many disease processes like edema, necrosis, or inflammation.[16,17]

Diverse pathological conditions have been studied using fetal brain ADC measurement so far. For example, compared with controls, ADC values in the brain fetuses with severe intrauterine growth restriction have been shown to be different.[18] Changes of ADC values in different fetal brain regions in CMV infection have also been described.[10,19]

The knowledge of normal and pathological MR signal due to changing tissue composition at a given time of the fetal

Table 1. Group Assignment and Characteristics

Group	Number of cases	Mean gestational age (weeks)
1. Control Group	143	28.15
2. Hydrocephalus/Ventriculomegaly	27	28.11
3. Ischemia/Hemorrhage	16	25.63
4. Infections	8	28.38
5. Congenital Diaphragmatic Hernia	14	30.36
6. Congenital Heart Disease	8	32.50

maturation is essential to adequately assess the imaging results, identify pathologies, and, in selected cases, initiate appropriate management.

The aim of this study was to investigate the development of ADC values in different brain areas in singleton fetuses affected by different intra- or extracranial pathologies in comparison with fetuses with normal brains.

Methods

Patient Data and Ethical Standards

This retrospective study was performed in accordance with the ethical standards and approved by the Institutional Review Board (Kantonale Ethikkommission für die Forschung Bern, Bern, Switzerland: 2016-00727) and with the 1964 Helsinki declaration and its later amendments or comparable ethical standards. An informed consent of the patients was waived due to the retrospective study design. The patients were referred to our department for fetal MR imaging after prenatal sonography suggested intra- or extracranial anomalies (eg, suspected brain or spine malformations, hydrocephalus, heart defect, diaphragmatic hernia, urogenital anomalies, etc; see Table 1), to rule out anomalies in cases of suspected prenatal infection or in a few cases – after previous pathological pregnancy.

Data regarding maternal health and when available, umbilical artery (UA) Doppler as well as cranial ultrasound findings of the fetuses with pathologies were retrospectively reviewed.

MR Protocol and Post Processing

We retrospectively reviewed all studies including DWI as part of the fetal MR imaging protocol from March 2005 to June 2016. DWI was performed on 1.5 T Magnetom Sonata or Magnetom Aera Siemens scanners (Siemens, Erlangen, Germany) with a single-shot spin-echo echo-planar axial DWI sequence acquired by use of a b-value of 0, 500, and 700 s/mm^2 in 3 orthogonal directions without sedation of the mother or fetus.

The application of gradients oriented in 3 planes in space using b-values between 0 and 700 s/mm^2 was chosen, since it is a part of many fetal imaging protocols,[14,20-22] where b-values between 400 and 700 s/mm^2 are considered to demonstrate optimal contrast in the fetal brain.[20]

The ADC maps were automatically calculated from the Siemens software. The following parameters were used: TR 4500 ms; TE 84 ms; FOV 320 mm; matrix 128 × 128 mm; section thickness 5 mm; skip 30% (1.5 mm); and bandwidth 1562 Hz.

The scan time of the diffusion sequence was 68 seconds, with overall examination time between 20 and 30 minutes. Sequences that could not be assessed due to motion or other types of artifacts and of poor image quality were excluded ($n = 27$ from an initial population of 381 fetuses, with a dropout rate of 8,5%). A total of 75 fetuses with cerebral malformations were identified. Due to the extreme heterogeneity of the pathologies (eg, Dandy-Walker malformation, agenesis of the corpus callosum, polymicrogyria, tuberous sclerosis, cystic malformations, holoprosencephaly, etc), this group was excluded for further analysis, since no general statement regarding the ADC values based on such inhomogeneous population can be made, resulting in a final population of 216 fetuses.

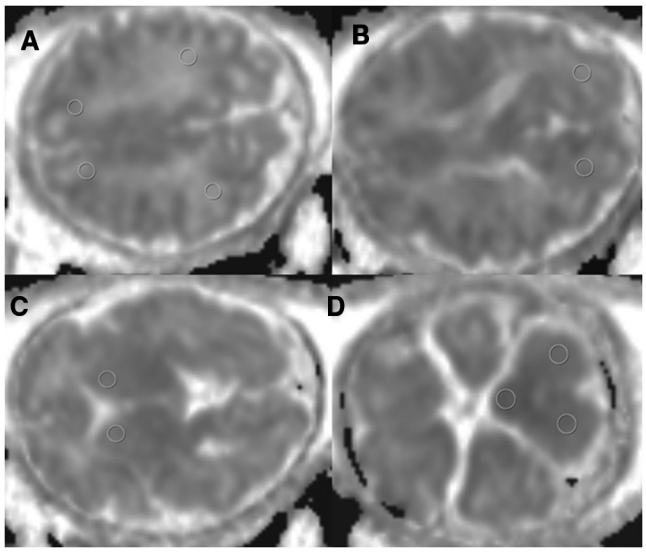

Fig 1. Placement of the ROIs on the ADC map. Images from the control group, 33 weeks gestational age. A) paired ROIs in the frontal and parietal white matter (WM); B) paired ROIs in the occipital WM; C) paired ROIs n the basal ganglia; D) single ROI in the middle of the pons; paired ROIs in the cerebellum.

A total of 11 circular regions of interest (ROIs) were placed on the ADC maps by a fellow radiologist (NSc), always under the supervision of senior pediatric neuroradiologists (CW, NSl) using Olea Sphere® software (Version 2.3, Olea Medical®) as follows: bilaterally in the WM of the frontal, parietal and occipital lobes, in the basal ganglia (BG), in the WM of the cerebellum and 1 ROI in the middle of the pons. ROIs placed in the supratentorial WM included the intermediate zone and the subplate zone (Fig 1). The size of the ROIs was adjusted for gestational age (GA).

Statistical Analysis

For all statistical analysis, a p-value ≤ .05 two-sided was considered statistically significant. The graphics were prepared using Microsoft Excel Software (2013) and SPSS (Version 21; IBM, Armonk, New York). ADC values of the groups with disease were compared to the control group using the nonparametric Mann-Whitney U-test due to group size differences. ADC values were correlated with GA using Spearman correlation.

Results

Group Assignment and Characteristics

All fetuses were assigned to 6 groups

A Student's t-test was performed for each side to compare the ADC values for each area and did not show any significant differences between the values of the right and left hemisphere

(all $p > .05$). Therefore, the mean values for each anatomical ROI location of the 2 hemispheres were included for further analysis, except for the ROI in the middle of the pons, where a single central measurement was performed (see Table 2).

The control group contained 143 fetuses with GA post menstruation between 14 and 40 weeks (mean 28.05 weeks). Of them, 57 had normal MRI findings and 86 had extracerebral pathologies, which were considered not interfering with brain development (for details and main indications for the studies please see Table 3).

The second group contained 27 cases of hydrocephalus ($n = 17$) or ventriculomegaly ($n = 10$) at a GA between 22 and 35 weeks (mean, 28.11 weeks).

The group of ischemia and/or hemorrhage contained 16 cases aged between 14 and 35 weeks GA (mean 25.63 weeks). Six fetuses suffered from cerebral ischemia, 9 from hemorrhage, and 1 fetus had both pathologies.

In total, 8 fetuses with congenital infections were examined between the 23rd and 34th gestational week (mean 28.38 weeks GA), of them 3 cases of cytomegalovirus (CMV) seroconversion, 2 cases of toxoplasmosis, and 3 cases with suspected TORCH infection based on radiological signs.

Our study included 12 cases of congenital diaphragmatic hernia (CDH), a case of massive pleural effusion, and a case of a chylothorax, all evaluated in the same group ($n = 14$) due to the identical effect of the pathology on the heart with mediastinal shift. The fetuses were examined between 24 and 37 weeks GA (mean 30.36 weeks).

In total, 8 fetuses with congenital heart disease (CHD) with a GA between 21 and 37 weeks (mean 32.5 weeks) were included. They suffered from an atrioventricular septal defect ($n = 2$), hypoplastic left heart syndrome ($n = 2$), cardiomegaly ($n = 1$), cardiac rhabdomyoma ($n = 1$), univentricular heart ($n = 1$), and a complex cardiac malformation with valve atresias and ventricular septal defect ($n = 1$).

Our population of fetuses with different intra- and extracranial pathologies ($n = 73$) included fetuses with normal and abnormal UA Doppler. In our series, 17% fetuses presented an abnormal UA Doppler (for details regarding pathological UA Doppler and fetal cranial ultrasound findings as well as maternal risk factors, please see Table 4).

Control Group

In the control group, the highest (mean) ADC values were measured in the frontal WM (1763.42×10^{-6} mm^2/s), followed by the parietal (1773.15×10^{-6} mm^2/s) and occipital WM (1723.34×10^{-6} mm^2/s); intermediate ADC values were measured in the BG and the cerebellum, and the lowest ADC values – in the pons (1309.43×10^{-6} mm^2/s; Table 2).

The evolution of the ADC values showed a significant increase with progressing GA in the frontal WM ($r = .208$, $p = .01$). A decrease was observed in the pons ($r = -.254$, $p = .002$) and in the cerebellum ($r = -.371$, $p < .001$; Fig 2).

Hydrocephalus/Ventriculomegaly Group

The occipital WM showed the highest ADC values (1781.81×10^{-6} mm^2/s), the pons – the lowest (1323.56×10^{-6} mm^2/s; Table 2).

The values in the pons remained almost unchanged. All other regions but the cerebellum (with a non-significant

Table 2. Group Assignment and ADC Values

	Mean ADC value [$\times 10^{-6}$ mm^2 / s] ± SD					
	Frontal WM	**Parietal WM**	**Occipital WM**	**Basal Ganglia**	**Cerebellum**	**Pons**
Control $n = 143$	1763.42 ± 221.71	1773.15 ± 205.32	1723.34 ± 213.05	1359.71 ± 190.67	1497.17 ± 183.58	1309.43 ± 175.61
Hydrocephalus/Ventriculomegaly $n = 27$	1705.09 ± 236.74	1759.69 ± 205.32	1781.81 ± 404.11	1389.57 ± 205.56	1501.25 ± 164.00	1323.56 ± 249.17
Ischemia/Hemorrhage $n = 16$	1506.51* ± 368.46	1592.07 ± 369.44	1597.72 ± 345.72	1195.18* ± 260.52	1475.26 ± 295.61	1294.75 ± 513.88
Infection $n = 8$	1869.51 ± 172.34	1986.88* ± 212.47	2021.44* ± 318.60	1446.64 ± 251.85	1589.33 ± 216.76	1362.13 ± 227.51
Congenital diaphragmatic hernia $n = 14$	1765.99 ± 218.87	1877.21 ± 256.38	1796.07 ± 252.71	1459.31 ± 314.44	1468.85 ± 164.60	1251.07 ± 263.56
Congenital heart disease $n = 8$	1692.38 ± 221.71	1765.87 ± 183.88	1713.44 ± 218.99	1319.05 ± 139.37	1412.91 ± 194.76	1229 ± 137.58

Data represent mean ± standard deviation unless otherwise indicated. WM: white matter, n = number of cases, *$p < .05$ compared to controls (Mann-Whitney U-test)

Table 3. Main Indications of the Control Fetuses

Indicaton	Number of cases		
Evaluation of placenta and uterus	$n = 14$	– Rule out placenta increta/percreta	$n = 13$
		– Condition after laser ablation of giant placental chorangioma	$n = 1$
Evaluation of the brain/ Questionable sonographic abnormalities	$n = 43$	– Arachnoid cyst, megacisterna magna, promiment cavum septi pellucidi	$n = 8$
		– Twin pregnancy with single fetal death	$n = 3$
		– Sonographically suspected malformation, subsequent normal fetal MR imaging results	$n = 31$
		– Eye globe abnormality	$n = 1$
Previous pregnancy with brain abnormalities	$n = 3$		
Evaluation of the spine	$n = 3$	– Spinal malformation	$n = 2$
		– Myelomeningocele/lipomyelomeningocele without evidence of Chiari malformation	$n = 1$
Sacrococcygeal teratoma	$n = 3$		
Suspected thoracic pathology	$n = 23$	– Congenital pulmonary airway malformation /Lung sequester	$n = 16$
		– Suspected congenital diaphragmatic hernia	$n = 5$
		– Intrathoracic space-occupying lesion	$n = 2$
Abdominal pathology	$n = 48$	– Kidney abnormalities	$n = 31$
		– Intestinal pathology	$n = 9$
		– Abdominal mass	$n = 5$
		– Abdominal wall defect	$n = 3$
Others	$n = 6$	– Sibling with pancreatic hypoplasia	$n = 1$
		– Situs inversus	$n = 1$
		– Neck cyst	$n = 2$
		– Mild hydrothorax	$n = 1$
		– Clubfoot	$n = 1$

n = number of cases

Table 4. Placenta Abnormalities and Maternal Health Factors

	Number of fetuses	Records available	Pathological umbilical Doppler	Abnormal fetal cranial ultrasound	Placental disorder (retroplacental hematoma, infarction)	Maternal health factors		
Group	*n*	*n* (%)	*n* (%)	*n* (%)	*n* (%)	Diabetes *n* (%)	Hyper-tension *n* (%)	Adipositas *n* (%)
Hydrocephalus/ Ventriculomegaly	27	15 (55.6)	0	0	0	3 (20)	0	2 (13.3)
Ischemia/Hemorrhage	16	15 (93.8)	7 (46.7)	11 (73.3)	4 (26.7)	0	0	0
Infections	8	7 (87.5)	0	4 (50)	0	0	0	0
Congenital diaphragmatic hernia	14	11 (78.6)	2 (18.2)	0	0	0	1 (7.1)	2 (14.2)
Congenital heart disease	8	5 (62.5)	0	0	0	0	0	0

n, number of cases.

decline) showed a non-significant increase in ADC values with increasing GA (for all tests: $r < .349$, $p > .07$). In the occipital WM the highest increase was found (Fig 3).

Ischemia/Hemorrhage Group

The highest ADC values were found in the occipital WM (1597.72×10^{-6} mm^2/s), the lowest – in the BG (1195.18×10^{-6} mm^2/s; Table 2). The frontal and parietal WM and the BG showed a non-significant increase with progressing GA (all $r > .325$, $p > .22$); the occipital WM, the cerebellum and the pons – a non-significant decrease (all $r < .48$, $p > .057$).

Infections Group

The highest ADC values were measured in the occipital WM (2021.44×10^{-6} mm^2/s), the lowest – in the pons (1362.13×10^{-6} mm^2/s; Table 2). The development of ADC values with progressing GA did not show any significant changes in any of the examined regions. A slight increase was observed in the

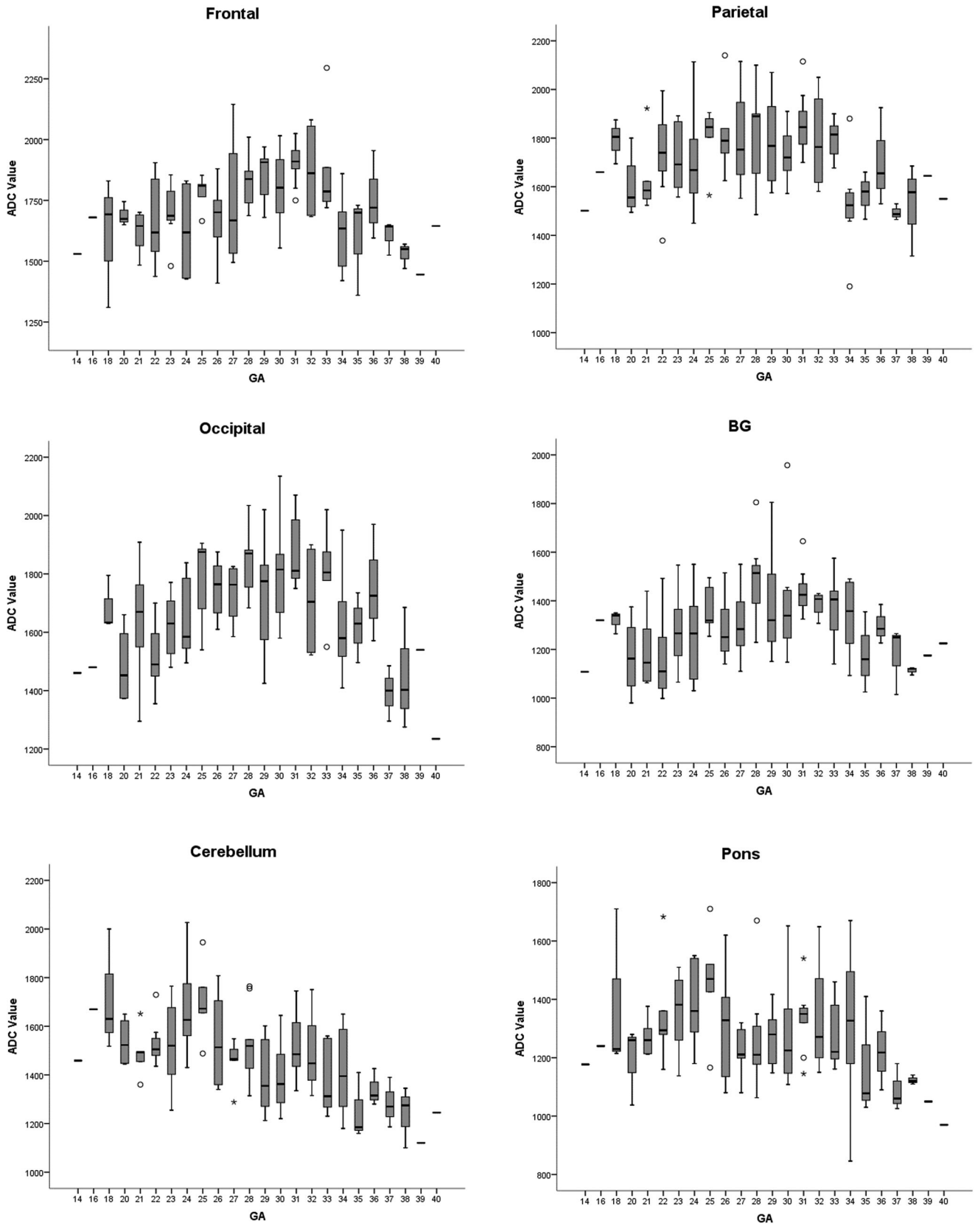

Fig 2. Distribution of the ADC values in different areas of the fetal brain with increasing gestational age in the control group. ADC value: ADC [$\times 10^{-6}$ mm^2/s]; GA: gestational age in weeks.

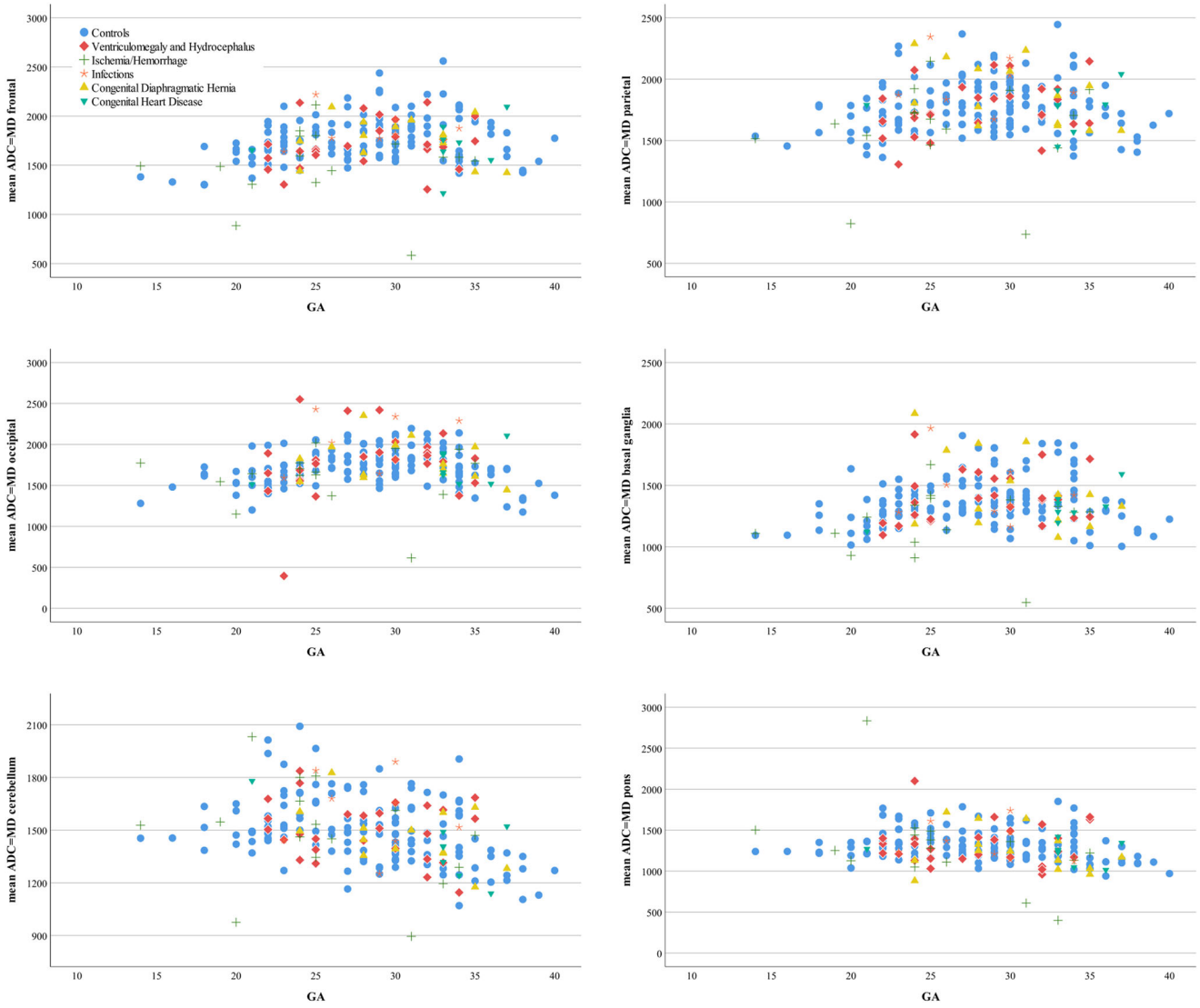

Fig 3. Distribution of the ADC values in different areas of the fetal brain with increasing gestational age. GA: gestational age in weeks, MD: mean diffusivity; ADC = MD [×10–6 mm2/s].

frontal and occipital WM, a slight decrease – in the remaining areas (Fig 3).

Congenital Diaphragmatic Hernia Group

The parietal WM showed the highest ADC values (1877.21 × 10^{-6} mm^2/s), the pons – the lowest (1251.07 × 10^{-6} mm^2/s; Table 2). Except for the parietal WM ($r = -.547$, $p = .04$), the values in all other regions showed a non-significant decrease with progressing GA (Fig 3).

Congenital Heart Disease Group

The fetuses with CHD showed the highest ADC values in the parietal WM (1765.87 × 10^{-6} mm^2/s), the lowest – in the pons (1229.0 × 10^{-6} mm^2/s; Table 2). The course of the values with progressing maturation showed neither significant increase nor decrease (Fig 3).

Discussion

Control Group

Considering the physiological maturation gradient with progressing myelination, the ADC values in the supratentorial WM are expected to be higher than in the cerebellum and the pons, and higher frontally than posteriorly. The development of the ADC values with progressing GA showed the expected decrease in the cerebellum and the pons, but not in the frontal and occipital WM and in the BG, each with a slight increase with advancing GA. Similar results have also been found in other studies[7] and could be explained by transient laminar compartments of the developing human brain,[23] for example, if the ROIs contain the subplate (a transient layer of the fetal brain, visible between the 22nd and 30th gestational week, and characterized by low cellular density). The radial expansion of the compartments at a specific time of the fetal development may explain the different course of the ADC values in healthy fetuses across studies.

Hydrocephalus/Ventriculomegaly Group

Hydrocephalus is one of the most common congenital anomalies. This disorder, which is characterized with a disturbance of cerebrospinal fluid (CSF) circulation resulting from an obstruction to the ventricular drainage system and CSF flow or a reduced CSF resorption, must be distinguished from ventriculomegaly, caused by loss of tissue, for example, in the case of agenesis of the corpus callosum, Arnold-Chiari malformations or holoprosencephaly, or as a result of periventricular leukomalacia.[11,24,25] Furthermore, the pathology can be divided into congenital cases, for example, in cases of Dandy-Walker malformations or Chiari Type II malformation, and in acquired pathologies, for example, as a result of infections or bleeding. In addition to etiology, early formation, cortical thickness of less than 1.5 mm, and loss of stratification on T2- and diffusion-weighted imaging are expected to be prognostically important.[24] The parenchymal compression caused by increased CSF pressure leads to reduced perfusion and ischemia with reduced ADC values of the cerebral parenchyma.[11,26-28]

In our study, lower ADC values were only found in the frontal WM, while all other values were higher compared to the control group.

The higher values as well as their increase with advancing GA may be explained by the time of imaging: in early stages of hydrocephalus, the ADC values rise due to CSF diapedesis into the parenchyma and decrease again after longer exposure to ischemia.[11,28,29] Another factor may be a delayed myelination.[30]

Ischemia/Hemorrhage Group

Ischemia is a common cause of fetal death.[25] The 20.4% of children who died in utero or during the neonatal period had evidence of prenatal ischemic brain damage in neuropathological studies.[25] The assessment of acute hypoxic lesions in adults is 1 of the main application of diffusion imaging.[31] The resulting cytotoxic edema restricts the extracellular diffusion and the ADC values decrease.

The pathophysiological changes following hypoperfusion/hypoxia explain the lower ADC values in all brain regions but pons and cerebellum in this groupcompared to controls. The transient laminar compartments of the developing WM explain their specific spatial and temporal vulnerability since those structures that are in a phase of intense growth at the time of a hypoxic-ischemic or hemorrhagic event are particularly sensitive.[23] The lowest ADC values in the BG can be explained by their selective vulnerability to ischemia-hypoxia.[32] The developing WM also experiences specific spatial and temporal vulnerability.[23,32-35] The expected decrease of the ADC values did not appear in the frontal and parietal WM and in the BG. A possible explanation is that it could be due to a more advanced tissue damage to these regions.

Infections Group

TORCH infections can lead to microcephaly, cerebellar hypoplasia, ventriculomegaly/hydrocephalus, calcifications, cysts, hemorrhage, and disorders of cortical development.[10,25,36,37]

The ADC values of the fetal brains in this group were higher in all regions than in the control group, especially in the parietal and occipital WM. Three fetuses were examined for CMV seroconversion. This virus is transmitted intrauterinely in 2.5% of all newborns and may lead to microcephaly, cerebellar hypoplasia, ventriculomegaly, and disorders of cortical development during the first and second trimesters due to affection of the subventricular and ventricular zones, the origin of the neuronal and glial cells.[10] Subependymal cysts, calcifications, and signal changes in the temporal lobe have typically been described in CMV infections.[38]

Other fetuses in this group of our study suffered from hepatomegaly with or without ascites. In contrast to the study by Yaniv et al.[10] who showed reduced ADC values in all brain regions of CMV infected fetuses, our population showed higher values compared to the control group. We hypothesize that this phenomenon could be explained by the time of intrauterine infection (early or late) or may represent chronic damage and WM gliosis, since a decrease in ADC values due to hypercellularity, inclusion bodies, and cytotoxic edema due to damage of the umbilical cord by the virus is expected only in the acute infection setting. Similar results as in the aforementioned study were obtained in the analysis of the development of ADC values with progressing gestational age, demonstrating decreasing ADC values in all regions except for the frontal and occipital WM.

Another fetus of our study suffered from a toxoplasmosis infection. On imaging, agenesis of the corpus callosum, microcephaly, and a delay of the cerebral maturation was found. In another fetus, an infection with the same pathogen was suspected due to the presence cerebral lesions (germinal matrix bleeding, hydrocephalus, focal gyration disorder/polymicrogyria). Characteristic cerebral lesions of the fetal toxoplasmosis infection are reduction of the parenchymal volume, calcifications of the BG, thalami, in the periventricular parenchyma, the cortex, the meninges, and the eyes.[25,37] As a consequence of obliteration of the mesencephalic aqueduct, hydrocephalus may occur.

Congenital Diaphragmatic Hernia Group

CDH has an incidence of 1 in 2,500 live births, with predominant left-sided defects (85%). The intrathoracic herniation of abdominal organs can lead to a shift of the mediastinum, the lungs, and the heart, with heart compression and compromise of the cerebral blood flow.[39] Depending on the size of the defect, the degree of lung hypoplasia and pulmonary hypertension, it is associated with high morbidity and mortality.[40,41] In previous studies, brain pathologies such as cortical malformations, intracranial bleeding, dilated external CSF spaces, and WM damage were detected in up to 60% of children with CDH.[40-44] The increased incidence of PVL in children with congenital diaphragmatic hernia is indicative of the high vulnerability of the WM in this population.[41] The neurological damage could be attributed to the significantly reduced cerebral blood flow.

In none of the fetuses with CDH examined in our study obvious morphological abnormalities were seen. This may be due to the timing of imaging before birth, as newborns who are postnatally treated with extracorporeal membrane oxygenation (ECMO), inotropic drugs, mechanical ventilation or a gastric tube, or are not orally fed, have an increased incidence of sequelae or neurolodevelopmental disorders,[40,41,44] "... likely as a result of treatments and therapies."[43]

Congenital Heart Disease Group

CHD are accompanied by high morbidity and global developmental disorders.[45] Newborns with CHD show changes in cerebral microstructure as a result of the deficient intrauterine oxygen and substrate supply.[45,46] Many of these children show brain damage before corrective or palliative cardiac surgery,[47] such as ischemia, intracranial hemorrhage, WM injury, delayed brain maturation, and decreased brain volume.[47-51]

The similarity of the pathologies to that seen in premature infants suggests comparable vulnerability due to immaturity of the brain tissue with concomitant increased vulnerability of the oligodendrocyte progenitor cells.[47,52,53] Fetuses with CHD show a significant increase of water diffusivity in the WM tracts.[45] We observed similar changes, with an increase in the ADC values in all regions of the WM as well as in the BG. None of the fetuses in this group showed morphological brain abnormalities, but the development of ADC values deviating from the control group is suggestive of abnormal brain maturation.

Some limitations have to be mentioned. The direct comparison of studies on the development of ADC values during the brain maturation process is limited due to the use of different MR systems and the different study populations with regard to their size and GA. The statistical power of our study is limited by the slab thickness and the resultant low spatial resolution of the ADC maps. As known, in some cases the quality of the DWI is also influenced by fetal or maternal motion. In our study, in the group of fetuses with CHD, only a small number of pathologies were present, so no general statement about the influence of congenital heart defects on the cerebral development can be made. Infants with CDH can suffer from brain damage resulting from postnatal therapies, which influence is not shown by prenatal imaging. The prognostic value of the observed ADC changes in the different groups of our study is still unknown, further studies and correlation with perinatal outcome are needed.

Regarding ADC estimation, the b-values for diffusion weighting have to be carefully chosen. Using a baseline b-value of 50 s/mm² in diffusion-weighted imaging instead of $b = 0$ in future studies may be more appropriate in order to eliminate contamination of the images from microperfusion.[54] Besides, the selection of b-values could be optimized and should be made depending on the expected MD of the parenchyma.[55]

To summarize, fetal diffusion MR imaging is a feasible method of detecting abnormal brain diffusivity associated with early microstructural impact of different pathologies on the developing brain.

Both the ADC values and their evolution curve in diseased fetuses are influenced and deviate from the expected course. Further in utero studies by using advanced MR imaging techniques with larger number of fetal populations in the particular disease groups are needed.

References

1. Schneider JF, Confort-Gouny S, Le Fur Y, et al. Diffusion-weighted imaging in normal fetal brain maturation. Eur Radiol 2007;17:2422-9.
2. Girard NJ, Chaumoitre K. The brain in the belly: what and how of fetal neuroimaging? J Magn Reson Imaging 2012;36:788-804.
3. Righini A, Bianchini E, Parazzini C, et al. Apparent diffusion coefficient determination in normal fetal brain: a prenatal MR imaging study. AJNR Am J Neuroradiol 2003;24:799-804.
4. Girard N, Chaumoitre K, Chapon F, et al. Fetal magnetic resonance imaging of acquired and developmental brain anomalies. Semin Perinatol 2009;33:234-50.
5. Schneider MM, Berman JI, Baumer FM, et al. Normative apparent diffusion coefficient values in the developing fetal brain. AJNR Am J Neuroradiol 2009;30:1799-803.
6. Manganaro L, Perrone A, Savelli S, et al. Evaluation of normal brain development by prenatal MR imaging. Radiol Med 2007;112:444-55.
7. Cannie M, De Keyzer F, Meersschaert J, et al. A diffusion-weighted template for gestational age-related apparent diffusion coefficient values in the developing fetal brain. Ultrasound Obstet Gynecol 2007;30:318-24.
8. Kasprian G, Del Rio M, Prayer D. Fetal diffusion imaging: pearls and solutions. Top Magn Reson Imaging 2010;21:387-94.
9. Boyer AC, Goncalves LF, Lee W, et al. Magnetic resonance diffusion-weighted imaging: reproducibility of regional apparent diffusion coefficients for the normal fetal brain. Ultrasound Obstet Gynecol 2013;41:190-7.
10. Yaniv G, Hoffmann C, Weisz B, et al. Region-specific reductions in brain apparent diffusion coefficient in cytomegalovirus-infected fetuses. Ultrasound Obstet Gynecol 2016;47:600-7.
11. Erdem G, Celik O, Hascalik S, et al. Diffusion-weighted imaging evaluation of subtle cerebral microstructural changes in intrauterine fetal hydrocephalus. Magn Reson Imaging 2007;25:1417-22.
12. Drobyshevsky A, Derrick M, Prasad PV, et al. Fetal brain magnetic resonance imaging response acutely to hypoxia-ischemia predicts postnatal outcome. Ann Neurol 2007;61:307-14.
13. Sartor A, Arthurs O, Alberti C, et al. Apparent diffusion coefficient measurements of the fetal brain during the third trimester of pregnancy: how reliable are they in clinical practice? Prenat Diagn 2014;34:357-66.
14. Jouannic JM, Blondiaux E, Senat MV, et al. Prognostic value of diffusion-weighted magnetic resonance imaging of the fetal brain in fetal growth restriction: results of a prospective multicenter study. Ultrasound Obstet Gynecol 2019 [Epub ahead of print].
15. Fabiano AJ, Horsfield MA, Bakshi R. Interhemispheric asymmetry of brain diffusivity in normal individuals: a diffusion-weighted MR imaging study. AJNR Am J Neuroradiol 2005;26:1089-94.
16. Alexander AL, Hurley SA, Samsonov AA, et al. Characterization of cerebral white matter properties using quantitative magnetic resonance imaging stains. Brain Connect 2011;1:423-46.
17. Clark KA, Nuechterlein KH, Asarnow RF, et al. Mean diffusivity and fractional anisotropy as indicators of disease and genetic liability to schizophrenia. J Psychiatr Res 2011;45:980-8.
18. Arthurs OJ, Rega A, Guimiot F, et al. Diffusion-weighted magnetic resonance imaging of the fetal brain in intrauterine growth restriction. Ultrasound Obstet Gynecol 2017;50:79-87.
19. Kotovich D, Guedalia JSB, Hoffmann C, et al. Apparent diffusion coefficient value changes and clinical correlation in 90 cases of cytomegalovirus-infected fetuses with unremarkable fetal MRI results. AJNR Am J Neuroradiol 2017;38:1443-8.
20. Manganaro L, Bernardo S, Antonelli A, et al. Fetal MRI of the central nervous system: state-of-the-art. Eur J Radiol 2017;93:273-3.
21. Katorza E, Strauss G, Cohen R, et al. Apparent diffusion coefficient levels and neurodevelopmental outcome in fetuses with brain MR imaging white matter hyperintense signal. AJNR Am J Neuroradiol 2018;39:1926-31.
22. Manganaro L, Bernardo S, La Barbera L, et al. Role of foetal MRI in the evaluation of ischaemic-haemorrhagic lesions of the foetal brain. J Perinat Med 2012;40:419-26.
23. Kostovic I, Kostovic-Srzentic M, Benjak V, et al. Developmental dynamics of radial vulnerability in the cerebral compartments in preterm infants and neonates. Front Neurol 2014;5:139.
24. Prayer D. Fetal MRI. Top Magn Reson Imaging 2011;22:89.
25. Prayer D. *Fetal MRI.* Heidelberg: Springer. 2011:287-327.
26. Braun KP, Dijkhuizen RM, de Graaf RA, et al. Cerebral ischemia and white matter edema in experimental hydrocephalus: a combined in vivo MRI and MRS study. Brain Res 1997;757:295-8.

27. Hidaka M, Matsumae M, Yamamura M, et al. Glucose metabolism and protective biochemical mechanisms in a rat brain affected by kaolin-induced hydrocephalus. Childs Nerv Syst 1997;13:183–8.
28. Gass A, Niendorf T, Hirsch JG. Acute and chronic changes of the apparent diffusion coefficient in neurological disorders–biophysical mechanisms and possible underlying histopathology. J Neurol Sci 2001;186 (Suppl 1):15-23.
29. Sotak CH. Nuclear magnetic resonance (NMR) measurement of the apparent diffusion coefficient (ADC) of tissue water and its relationship to cell volume changes in pathological states. Neurochem Int 2004;45:569-2.
30. von Koch CS, Gupta N, Sutton LN, Sun PP. In utero surgery for hydrocephalus. Childs Nerv Syst 2003;19:574-86.
31. Schaefer PW, Copen WA, Lev MH, Gonzalez RG. Diffusion-weighted imaging in acute stroke. Neuroimaging Clin N Am 2005;15:503-30.
32. Sie LT, van der Knaap MS, Oosting J, et al. MR patterns of hypoxic-ischemic brain damage after prenatal, perinatal or postnatal asphyxia. Neuropediatrics 2000;31:128-36.
33. Miller SP, Ferriero DM. From selective vulnerability to connectivity: insights from newborn brain imaging. Trends Neurosci 2009;32:496-505.
34. Volpe JJ. Brain injury in premature infants: a complex amalgam of destructive and developmental disturbances. Lancet Neurol 2009;8:110-24.
35. Mathur A, Inder T. Magnetic resonance imaging–insights into brain injury and outcomes in premature infants. J Commun Disord 2009;42:248-55.
36. Engman ML, Lewensohn-Fuchs I, Mosskin M, Malm G. Congenital cytomegalovirus infection: the impact of cerebral cortical malformations. Acta Paediatr 2010;99:1344-49.
37. Barkovich AJ, Girard N. Fetal brain infections. Childs Nerv Syst 2003;19:501-7.
38. Doneda C, Parazzini C, Righini A, et al. Early cerebral lesions in cytomegalovirus infection: prenatal MR imaging. Radiology 2010;255:613-21.
39. DeKoninck P, Richter J, Van Mieghem T, et al. Cardiac assessment in fetuses with right-sided congenital diaphragmatic hernia: case-control study. Ultrasound Obstet Gynecol 2014;43:432-6.
40. Radhakrishnan R, Merhar S, Meinzen-Derr J, et al. Correlation of MRI brain injury findings with neonatal clinical factors in infants with congenital diaphragmatic hernia. AJNR Am J Neuroradiol 2016;37:1745-51.
41. Danzer E, Zarnow D, Gerdes M, et al. Abnormal brain development and maturation on magnetic resonance imaging in survivors of severe congenital diaphragmatic hernia. J Pediatr Surg 2012;47:453-61.
42. Hunt RW, Kean MJ, Stewart MJ, Inder TE. Patterns of cerebral injury in a series of infants with congenital diaphragmatic hernia utilizing magnetic resonance imaging. J Pediatr Surg 2004;39:31-6.
43. Tracy S, Estroff J, Valim C, et al. Abnormal neuroimaging and neurodevelopmental findings in a cohort of antenatally diagnosed congenital diaphragmatic hernia survivors. J Pediatr Surg 2010;45:958-65.
44. Ahmad A, Gangitano E, Odell RM, et al. Survival, intracranial lesions, and neurodevelopmental outcome in infants with congenital diaphragmatic hernia treated with extracorporeal membrane oxygenation. J Perinatol 1999;19:436-40.
45. Miller SP, McQuillen PS, Hamrick S, et al. Abnormal brain development in newborns with congenital heart disease. N Engl J Med 2007;357:1928-38.
46. Donofrio MT, Bremer YA, Schieken RM, et al. Autoregulation of cerebral blood flow in fetuses with congenital heart disease: the brain sparing effect. Pediatr Cardiol 2003;24:436-43.
47. Owen M, Shevell M, Majnemer A, Limperopoulos C. Abnormal brain structure and function in newborns with complex congenital heart defects before open heart surgery: a review of the evidence. J Child Neurol 2011;26:743-55.
48. Mahle WT, Tavani F, Zimmerman RA, et al. An MRI study of neurological injury before and after congenital heart surgery. Circulation 2002;106:109-14.
49. McQuillen PS, Barkovich AJ, Hamrick SE, et al. Temporal and anatomic risk profile of brain injury with neonatal repair of congenital heart defects. Stroke 2007;38:736-41.
50. Sun L, Macgowan CK, Sled JG, et al. Reduced fetal cerebral oxygen consumption is associated with smaller brain size in fetuses with congenital heart disease. Circulation 2015;131:1313-23.
51. Barbu D, Mert I, Kruger M, Bahado-Singh RO. Evidence of fetal central nervous system injury in isolated congenital heart defects: microcephaly at birth. Am J Obstet Gynecol 2009;201:41-7.
52. Miller SP, McQuillen PS, Vigneron DB, et al. Preoperative brain injury in newborns with transposition of the great arteries. Ann Thorac Surg 2004;77:1698-706.
53. McQuillen PS, Miller SP. Congenital heart disease and brain development. Ann N Y Acad Sci 2010;1184:68-86.
54. Dijkstra H, Baron P, Kappert P, et al. Effects of microperfusion in hepatic diffusion weighted imaging. Eur Radiol 2012;22:891-9.
55. Gillard J, Waldman A, Barker P. *Clinical MR Neuroimaging: Diffusion, Perfusion and Spectroscopy.* Cambridge, England: Cambridge University Press; 2005.